Original article

Med Lasers 2024;13(1):35-46
https://doi.org/10.25289/ML.24.004
pISSN 2287-8300 · eISSN 2288-0224

MEDICAL LASERS
Engineering Basic Research and Clinical Application

Original article

Multiple-wavelength radiation promotes hair growth by enhancing the early stages of hair follicle development in human dermal papilla cells and C57BL/6 mice

Soo Min Kim[1], Tae-Rin Kwon[1], Dong Wook Moon[1], Jungwook Kim[1], Rae Hyun Lim[1], Jungkwan Lee[1], So Young Lee[2], Ka Ram Kim[2], Young Gue Koh[2], Hye Sung Han[3], Sun Young Choi[3], Kwang Ho Yoo[3]

[1]*Home Beauty Development Team, Home Appliance & Air Solution, LG Electronics, Seoul, Republic of Korea*
[2]*Department of Dermatology, Chung-Ang University Hospital, Seoul, Republic of Korea*
[3]*Department of Dermatology, Chung-Ang University Gwangmyeong Hospital, Chung-Ang University College of Medicine, Gwangmyeong, Republic of Korea*

Background: We aimed to clarify the safety and efficacy of simultaneous skin exposure to blue, red, and infrared light. The purpose of this study was to confirm the mechanism by which multiple wavelengths increase hair development both in vivo and in vitro.

Methods: Cultured human dermal papilla cells (hDPCs) were exposed to a 470/655/850 nm light-emitting diode (LED) array with a fixed energy density of 3.0 mW/cm^2. We analyzed alkaline phosphatase (ALP) staining and activity. The relative expressions of *ALP*, *VEGF*, *Shh*, and *OPN3* were examined using reverse transcriptase-polymerase chain reaction arrays 48 hours post-exposure and the protein levels related to extracellular signal-regulated kinase (ERK)/protein kinase B (AKT)/glycogen synthase kinase 3 (GSK3)β signaling were assessed by western blotting. Next, we used H&E staining, hair growth scoring, skin thickness measurement, and the immunohistochemical analysis of the dorsal skin of C57BL/6 mice to investigate the effects of the mono- or combined-photobiomodulation (PBM) groups.

Results: According to our findings, simultaneous irradiation with multi-wavelength LEDs at 470/655/850 nm increased the proliferation of hDPCs. Also, compared to the control group, the red wavelength and combined PBM groups had significantly improved skin thickness measurements. Overall, we concluded that the combined PBM therapy successfully induced the early onset of anagen and stimulated hair growth.

Conclusion: These results suggest that PBM therapy regulates hair growth by activating the ERK/AKT/GSK3β signaling pathway. Thus, multiple-wavelength radiation from devices combining radiation emitted by low-power lasers and LEDs could be a new approach for promoting PBM-induced beneficial effects.

Key words: Low-level laser therapy; Photobiomodulation; Hair

INTRODUCTION

Photobiomodulation (PBM) relies on stimulation of cells by emitted radiation, and light-emitting diodes (LEDs) have been proposed as the foundation for the therapeutic effects on biological tissues. In regenerative

Received February 13, 2024, **Accepted** March 8, 2024

Correspondence
Kwang Ho Yoo
E-mail: psyfan9077@naver.com
ORCID: https://orcid.org/0000-0002-0137-6849

© Korean Society for Laser Medicine and Surgery
This is an open access article distributed under the terms of the Creative Commons Attribution Non-Commercial License (https://creativecommons.org/licenses/by-nc/4.0) which permits unrestricted non-commercial use, distribution, and reproduction in any medium, provided the original work is properly cited.

www.kci.go.kr

medicine, healthcare professionals, dentists, and laser therapists frequently use this low-risk, noninvasive technique to treat a range of ailments. PBM has analgesic effects, lessens inflammation, and encourages tissue repair [1].

PBM using diode lighting is growing in popularity from a business and aesthetic standpoint. The physiological underpinnings of this phenomenon, referred to as PBM, can be comprehended in terms of regulating inflammation, growth factor synthesis, mitochondria respiration, gene expression, and cell signaling [2].

The foundation of diodes is the electric luminescence phenomenon, which is the generation of light as a nonresistive result of electricity passing through a semiconductor material. In other words, the light is not a result of heat. They present no risk of retinal damage, so eye protection is unnecessary. Diodes can produce light at different wavelengths from the same power source. The fundamental components are cheap to create, and electrical luminescence can be generated with a comparatively tiny power source [3]. With portable and wearable devices that use LEDs instead of laser light, the foundation for most preclinical findings, PBM has become increasingly popular in clinical settings and at home [4].

The PBM effect depends on chromophores, or photoreceptors, absorbing incident radiation energy within cells. This process initiates photophysical and photochemical processes at the molecular and cellular levels. Physical characteristics of radiation, including wavelength, energy density, power density, emission mode (continuous wave or pulsed), irradiation time, irradiation mode, and clinical irradiation, all affect these processes. In addition, clinical and physical radiation parameters, including the number of irradiation points, the irradiation area, application approach, and treatment frequency, will also impact this phenomenon. Different areas of the body will target or absorb incident radiation in different ways, depending on the energy density and wavelength of the radiation. Therefore, compared to effects associated with mono-radiation, a combination of distinct radiations (different wavelengths) may have diverse effects on tissues, such as cell proliferation and differentiation [5].

The scientific community has taken notice of blue light (450-480 nm) and is using it in an increasing number of studies. Its key characteristics include lowering the release of proinflammatory cytokines, enhancing tissue hydration, reducing cellular processes, and having an anti-proliferative effect on human endothelial cells. It also promotes recovery from acute skin wounds. In general, findings vary, although positive results have been observed at various wavelengths in the red (600-700 nm) and near-infrared (NIR, 770-1,200 nm) spectral regions. Though research on blue and green wavelengths has recently started, penetration depth is an important challenge. Molecules and tissue structures absorb and scatter light, controlling how much of it enters the tissue [6-8].

The NIR penetration depth reaches its maximum at approximately 810 nm due to a large reduction in absorption and scattering at longer wavelengths, when water starts to play a significant role as an absorber, causing the penetration depth to decrease once more. Several patients are using these nonsurgical therapies; therefore, explaining the theoretical foundations of PBM to the patients and providing them with appropriate advice is critical. This review's objectives are to assess and compile the preclinical data supporting PBM and make recommendations about the substitution of diode light for laser light [9].

Our results demonstrate the possibility that PBM therapy may promote hair development by upregulating the expression of proliferative factors in hair follicles. Simultaneous exposure to different wavelengths promotes early hair growth and accelerates the growth cycle. These advancements are critical to understanding the hair growth cycle and creating more promising therapies for hair growth and loss.

METHODS

Ethics statement: All procedures involving animals were conducted following the guidelines of the Institutional Animal Care and Use Committee of CRONEX in Korea (no. 20220302).

Isolation and culture of human dermal papilla cells

Human dermal papilla cells (hDPCs) were purchased from Cefobio as primary cells and were grown in human dermal papilla growth medium (Cefogro-HDF; Cefobio) supplemented with 5% fetal bovine serum (FBS; Invitrogen/Gibco-BRL) and 1% penicillin in a humidified environment. Human follicular DPCs from the third or fourth passage were used.

Test module

The cell culture plate was placed under the LED device. The distance between the LED panel and the bottom of the cell culture plate was approximately 5 cm, and

www.kci.go.kr

the light irradiance could be adjusted from 3.0 mW/cm^2 through a current power supply. For the in vitro study, LEDs with wavelengths of blue LED 470 ± 5 nm (BL-HB535A-TRB; Bright LED Electronics Corp.), red LED 655 ± 5 nm (CTSRZ12A; Seoul Viosys), and infrared LED 850 nm (BIR-HO036A-TRB; Bright LED Electronics Corp.) were used as the low-level laser therapy (LLLT) sources. The light irradiances were 3.0 mW/cm^2, and the irradiation times were 9 and 18 minutes.

For the in vivo study, the LED/laser beam was delivered to the mouse dorsal skin region through direct irradiation using a dome-shaped module with an aperture of 20 mm [10]. All procedures were applied to all groups under the same conditions. The animals were randomly divided into eight groups (n = 5 per group): Group 1, untreated controls; Group 2, minoxidil (MXD), topical application (3% MXD; Hyundai Pharm), 0.2 ml, applied three times a week; Group 3, 470 nm LED 3 mW, 18 minutes three times a week; Group 4, 850 nm LED 3 mW, 18 minutes three times a week; Group 5, 650 nm LED/660 nm LD 3 mW, 18 minutes three times a week; Group 6, combine (470 + 850 + 650 nm LED/660 nm laser diode [LD]) 3 mW, 4.5 minutes three times a week; Group 7, combine (470 + 850 + 650 nm LED/660 nm LD) 3 mW, 9 minutes three times a week; and Group 8, combine (470 + 850 + 650 nm LED/660 nm LD) 3 mW, 18 minutes three times a week.

Alkaline phosphatase activity assay

Dermal papilla cells were trypsinized, and the cells were cultured in 96-well plates at a cell density of 2,500/well in 10% FBS–Dulbecco's modified Eagle medium (DMEM) containing various concentrations for 24 hours. For each irradiation of PBM, three wells of cell culture were used. The plate was incubated at 37°C for 2 hours to determine the cell count and seeding. The cell number was determined by measuring the absorbance at 450 nm, and then the reagent was removed, the well was rinsed with 100 μL of phosphate-buffered saline (PBS) twice, and the plate was subjected to three freeze (–80°C)/thaw cycles. Two hundred microliters of 1 mg/ml 4-nitrophenylphosphate bisalt (Sigma-Aldrich) in 1 M diethanolamine buffer (pH 9.8) were added to the well, and the plate was incubated at 37°C for 30 minutes and read at 405 nm to determine alkaline phosphatase (ALP) activity.

Real-time polymerase chain reaction

Total RNA from cultured hDPCs was prepared using Sepasol RNA (Nacalai Tesque) and reverse-transcribed with SuperScript III Reverse Transcriptase (Invitrogen) according to the manufacturer's instructions. The cDNA (>50 ng) thus obtained was used as a template for reverse transcriptase-polymerase chain reaction (PCR), which was carried out with AmpliTaq Gold DNA Polymerase (Applied Biosystems) for 35 cycles of 94°C for 30 seconds, 55°C for 60 seconds, and 72°C for 2 minutes using the primers listed below for amplification. Real-time PCR was performed using SYBR green Q-PCR master mix (Invitrogen) on the AB 7500 Real-Time PCR System (Applied Biosystems) under the following conditions: 45 cycles of 95°C for 15 seconds and 60°C for 1 minute. The sequences of the PCR primer sets used in this study are as follows: *shh* (accession no.: NM_000193; forward primer: CCGAGCGATTTAAGGAACTCACC, reverse primer: AGCGTTCAACTTGTCCTTACACC), *OPN3* (accession no.: NM_014322; forward primer: ATGGTCACCTGGTCACTCCAAC, reverse primer: GAGGCACAGAAGCTGCAAAAGG), *ALP* (accession no.: NM_014476; forward primer: GGTCAGGTTTCAACAGCCCTAG, reverse primer: GGTCAGGTTTCAACAGCCCTAG), *VEGF* (accession no.: NM_001025366; forward primer: TTGCCTTGCTGCTCTACCTCCA, reverse primer: GATGGCAGTAGCTGCGCTGATA).

Measurement of cytokine production

Vascular endothelial growth factor (VEGF) concentrations in culture supernatant from PBM irradiated hDPCs were determined using a commercially available ELISA kit according to the manufacturer's instructions (R&D Systems). The obtained supernatant of irradiated cells was centrifuged and collected to determine the production of VEGF. The absorbance was measured at 570 nm using an automatic microplate reader, and the VEGF concentration of each unknown sample was calculated using the standard curve. All samples and standards were measured in triplicate.

Western blotting

Cells were harvested and washed with ice-cold PBS. The cells were lysed in a radioimmunoprecipitation assay (RIPA) buffer containing 50 mM Tris pH 8.0, 150 mM NaCl, 0.1% SDS, 1% NP-40, 0.1% sodium deoxycholate, protease inhibitor cocktail (Roche), 1 mMNa3V04, 20 mM NaF, and 1 mM Na4P207. A total of 40 mg of total protein, quantified with a BCA kit (Pierce), were separated by sodium dodecyl sulfate-polyacrylamide gel electrophoresis (SDS-PAGE) and transferred to Protran (0.45 mm) nitrocellulose membranes (Schleicher & Schuell). The membranes were blocked with 5% milk in PBS and sub-

www.kci.go.kr

sequently incubated with the phosphor-extracellular signal-regulated kinase (ERK) antibody (#4695; Cell Signaling), p-phosphor-ERK antibody (#4370; Cell Signaling), protein kinase B (AKT) antibody (#9272; Cell Signaling), phosphor-AKT antibody (#9271; Cell Signaling), glycogen synthase kinase 3 (GSK3)β antibody (#9315; Cell Signaling), phosphor-GSK3β antibody (#9336, Cell Signaling) diluted at 1:1,000 for 3 hours at room temperature. After incubation with the secondary antibodies conjugated to horseradish peroxidase (1:2,000; Dako) for 1 hour, the bands were visualized by enhanced chemiluminescence (ECL) (Amersham Biosciences Europe).

Hair growth activity in vivo

In total, 40 6-week-old female C57BL/6J mice, Samtako Bio Korea, were randomly divided into eight groups (five mice/group). The degree of induction of the growth phase was evaluated by observing the change in skin color while the test module was applied for several weeks after the back hairs of C57BL/6 mice aged 6-7 weeks, in a resting state, were shaved. The dorsal hair of C57BL/6 mice has a time-synchronized growth cycle and stem pigmentation that occurs only in the anagen phase of hair growth.

Determination of hair growth-promoting activity

Photographs were taken on days 3, 10, 14, and 18 to record hair growth progress. The effect on hair growth in each group was scored as follows: 0%-19% (1 point), 20%-39% (2 points), 40%-59% (3 points), 60%-79% depending on the degree of hair growth by visually observing each animal (4 points), and 80%-100% (5 points). ImageJ (version 1.47, National Institutes of Health) was used to quantify the total hair growth and follicle count on day 18 from the photographs.

Quantitative histomorphometry

At the end of the test, the skin on the back was removed and fixed with 10% formalin. After dehydration with alcohol and xylene (step by step) and embedding in paraffin, 5 μm or less tissue sections were prepared using a microtome, and paraffin was removed again with alcohol and xylene. The epidermis was observed by staining with H&E, and skin thickness, which corresponds to hair follicle length [11] was defined as the distance between the granular layer of the epidermis and the panniculus carnosus. Each sample was tested in three different areas, and each mouse's average value was chosen.

Immunohistochemical staining

Immunohistochemical staining was performed using the UltraVision LP Large Volume Detection System HRP Polymer kit (Thermo Fisher Scientific). The primary antibodies used were sonic hedgehog (Shh, ab135240; Abcam) and Opsin-3 (OPN3, ab228748; Abcam). The paraffin was removed from sections using xylene and immersed in ethanol for rehydration. The sample was heated in 3% hydrogen peroxide for 10 minutes and washed four times with 1X Tris-buffered saline (TBS) to inhibit endogenous peroxidase activity. After reacting with Ultra V Block (Lab Vision; Thermo Fisher Scientific) at room temperature for 5 minutes, the primary antibody was uniformly added to each tissue and reacted at 4°C for 18 hours in a moist chamber to suppress non-specific reactions. After washing the slides, the primary antibody enhancer was allowed to react for 10 minutes, followed by the horseradish peroxidase (HRP) polymer for 15 minutes at room temperature. After washing, the slides were stained with 3,3'-diaminobenzidine (DAB) substrate for 10-30 seconds, counterstained with Mayer's hematoxylin, and sealed by dehydration. Two independent, blinded pathologists evaluated each serial section. Each pathologist assigned each section a score according to the following scale: 0, negative control; +, moderately increased staining; ++, considerably increased staining, based on the percentage of stained cells in each category [12].

Statistical analysis

For the analysis of in vivo results, IBM SPSS Statistics 26.0 (IBM Corp.) was used to perform statistical analysis on collected data. One-way ANOVA or paired t-tests were used for the statistical analysis of appropriate quantitative data. Otherwise, the Wilcoxon test was conducted for the nonparametric test. $p < 0.05$ was considered statistically significant.

For the analysis of in vivo results, trends were analyzed using figures for each period and group organized by means and standard errors. For comparison between the control and test groups, the p-value was calculated through ANOVA with SPSS, and a p-value of <0.05 was considered significant. Tukey multiple comparison was performed as a post-hoc analysis, and the indication was as follows: $p < 0.05$, $p < 0.01$, and $p < 0.001$.

RESULTS

Determination of cell growth and detection of ALP activity

To determine an irradiation range for investigating the

www.kci.go.kr

effects of 470/655/850 nm LED on hDPC viability, we used cells that were irradiated using a novel LED device for in vitro testing. Each power fluence of 3.0 mW/cm^2 was delivered to a platform 50 mm under the LED arrays (Fig. 1A). Before each LED irradiation, the cultures were rinsed in PBS and irradiated with the indicated

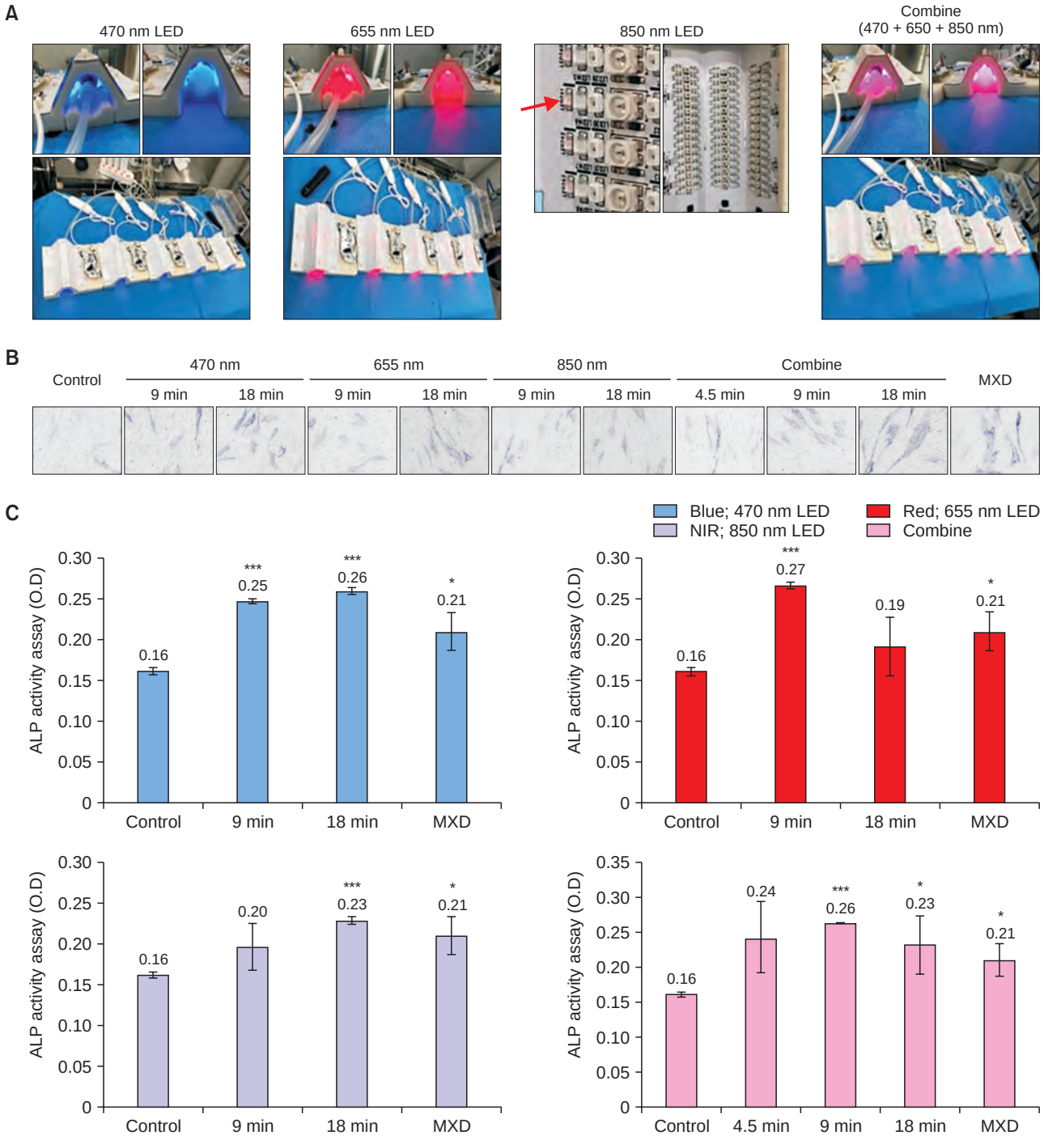

Fig. 1. Multiple-wavelength light-emitting diode (LED) radiation regulates the proliferation of human dermal papilla cells. (A) Wavelengths are often referred to using their associated color and include blue (470 nm), red (650/655 nm), and near-infrared (NIR) (850 nm) lights. The red arrow indicates violet color (NIR). (B) Alkaline phosphatase (ALP) staining (original magnification, ×100). Cell morphology (left panels) was examined under a bright-field microscope. Dark blue staining indicates ALP-expressing cells. (C) ALP activity for 48 hours (n = 3). Asterisks denote significant differences between control and test groups as measured by the t-test, with *$p < 0.05$ and ***$p < 0.001$. MXD, minoxidil.

www.kci.go.kr

fluencies in PBS to avoid absorption by the phenol-red in the culture medium. All groups were kept in PBS at room temperature during the experimental procedure to ensure equal treatment conditions. Proliferation assays showed that cell proliferation of hDPCs was significantly increased upon each LED irradiation (data not shown). Nearly all freshly isolated hDPCs express ALP activity, and most lose their ALP activity over the first several days in culture or passage. We decided to measure the levels of ALP expression in each PBM-irradiated and MXD-treated condition because it is a well-known dermal papilla cell marker. Furthermore, compared to the control group, the number of ALP-positive cells and ALP activity in the PBM irradiated group (Fig. 1B, C). These findings suggest that a single or a combination of PBM unknown factors may effectively maintain hDPC characteristics in vitro.

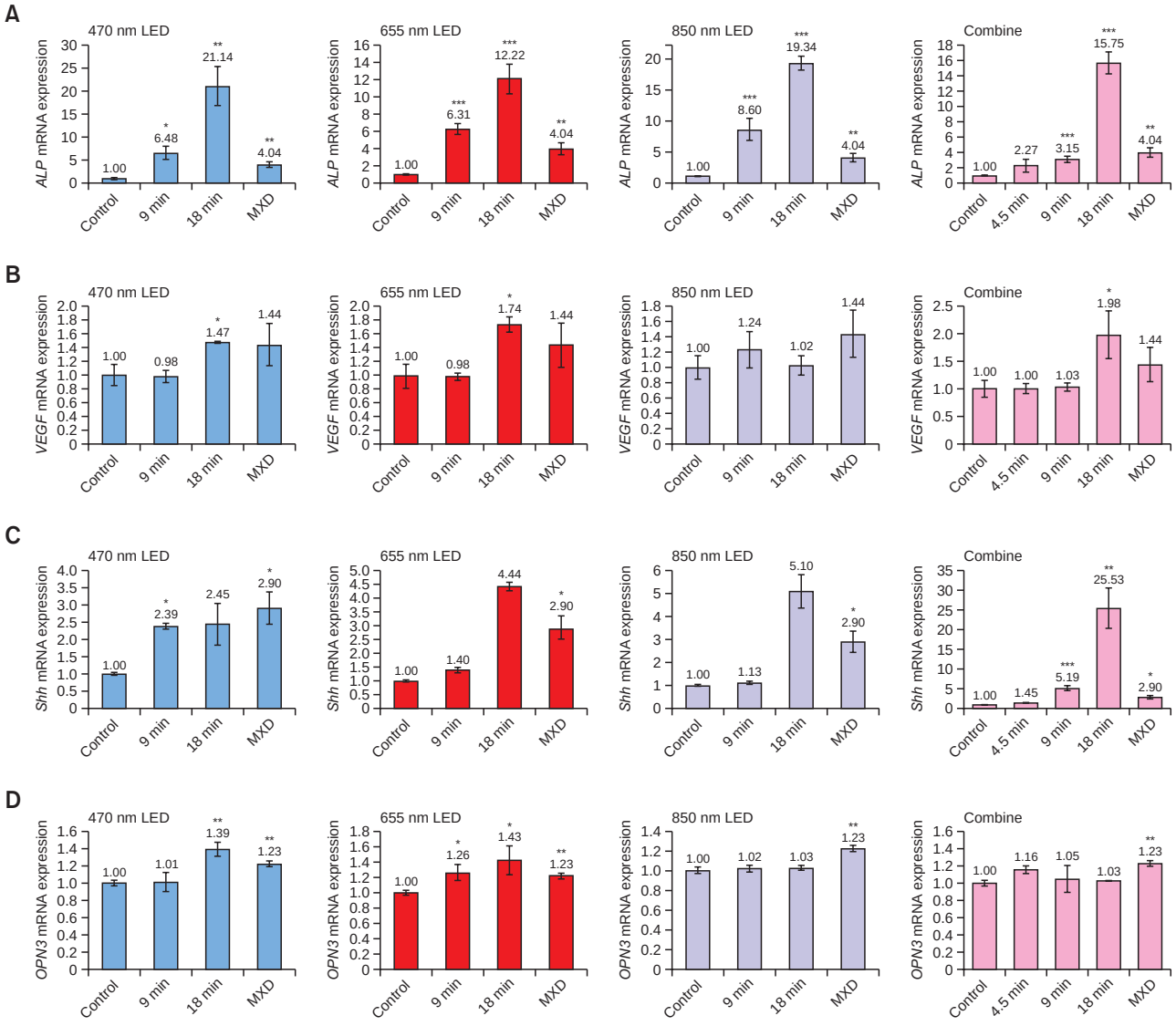

Fig. 2. Multiple-wavelength light-emitting diode (LED) enhances the inductive effects of human dermal papilla cells (hDPCs) on hair growth-related pathways. Real-time RT-PCR analysis of (A) alkaline phosphatase (*ALP*), (B) *VEGF*, (C) *Shh*, and (D) *OPN3* expression using total RNA prepared from LED-treated hDPCs. Effects of LED irradiation on the protein expression of ERK/AKT/GSK3β/signaling pathway in hDPCs. The hDPCs (2×10^5 cells/well) were cultured in serum-free Dulbecco's modified Eagle medium for 24 hours and then irradiated with indicated doses and wavelengths and incubated for (E) 2 hours and (F) 48 hours. The protein level of phosphorylated ERK/AKT/GSK3β was examined by Western blot and normalized against total form expression. The relative level is shown as mean ± standard deviation from triplicate samples. Values are shown as relative ratios. Statistically significant differences were determined by one-way ANOVA (*$p < 0.05$, **$p < 0.01$, ***$p < 0.001$) compared to control. mRNA, messenger RNA; MXD, minoxidil.

www.kci.go.kr

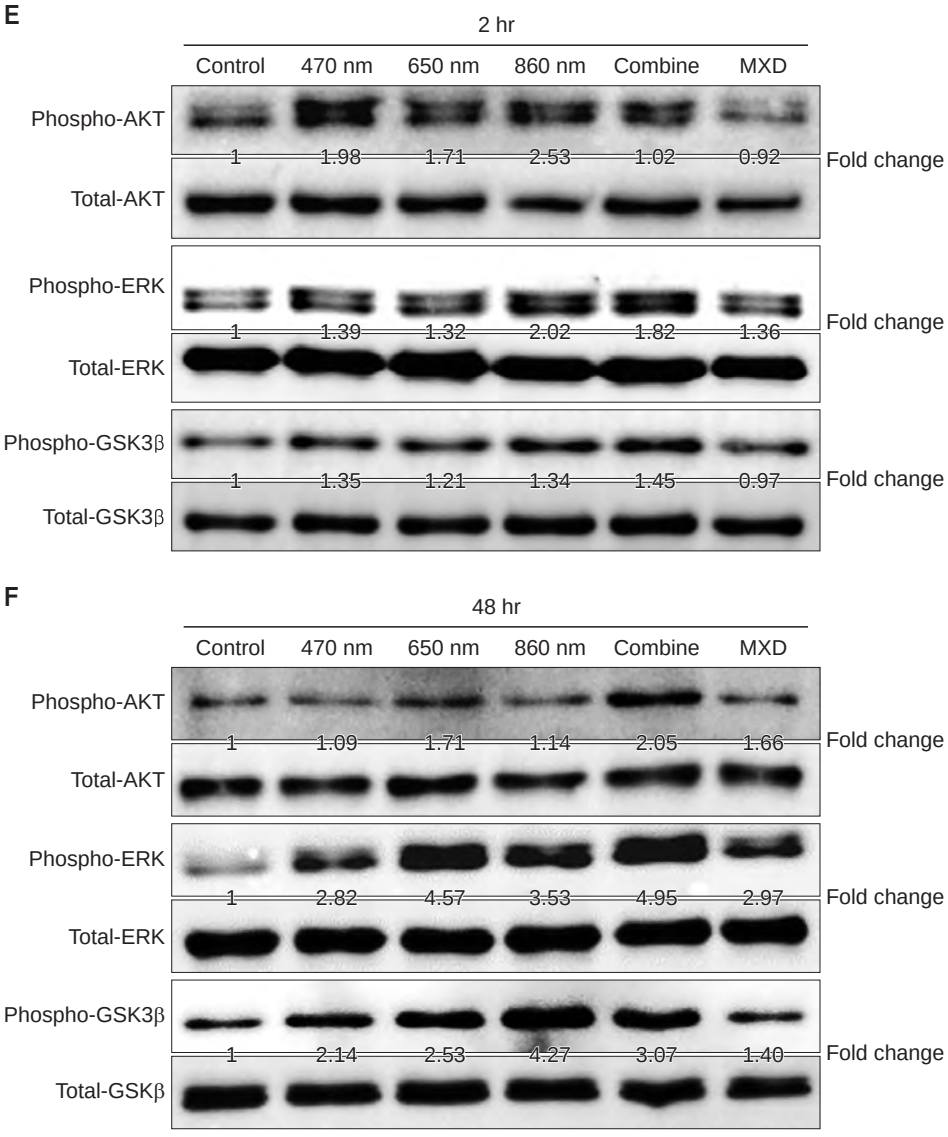

Fig. 2. Continued.

LED light promoted the proliferation of hDPCs by activating the ERK/AKT/GSK3β signaling pathway

Next, we examined changes in the messenger RNA (mRNA) expression of *ALP*, *VEGF*, *Shh*, and *OPN3*. Monoor combined-irradiation significantly increased *ALP* expression in an irradiation time-dependent manner. A 10-15-fold improvement at 470, 655, and 850 nm was observed at all doses. Also, the combined irradiation significantly increased *Shh* expression in an irradiation time-dependent manner. There was a 25-fold improvement in the combined group at all doses for 18 minutes (Fig. 2A-D).

We also measured the phosphorylated protein expressions of ERK, AKT, and GSK3β in hDPCs.

The results of Western blot analysis showed that proteins related to the hair follicle growth cycle activation significantly increased in each of the following groups: all groups irradiated with wavelengths of 470, 650, or 850 nm, the simultaneously irradiated group, and the positive control group treated with MXD. At 48 hours, the simultaneous irradiation group induced the highest peak expression of AKT phosphorylation (Fig. 2E, F). These results further confirmed that groups irradiated with each wavelength simultaneously worked synergistically to effectively promote hair follicles into the anagen phase.

Evaluation of morphological observation and hair growth rate

As a pigmented species, C57BL/6 mice were chosen for the subsequent hair regeneration experiment because the growth time of their hair follicles affects the color of their skin. We went with the conventional hair

www.kci.go.kr

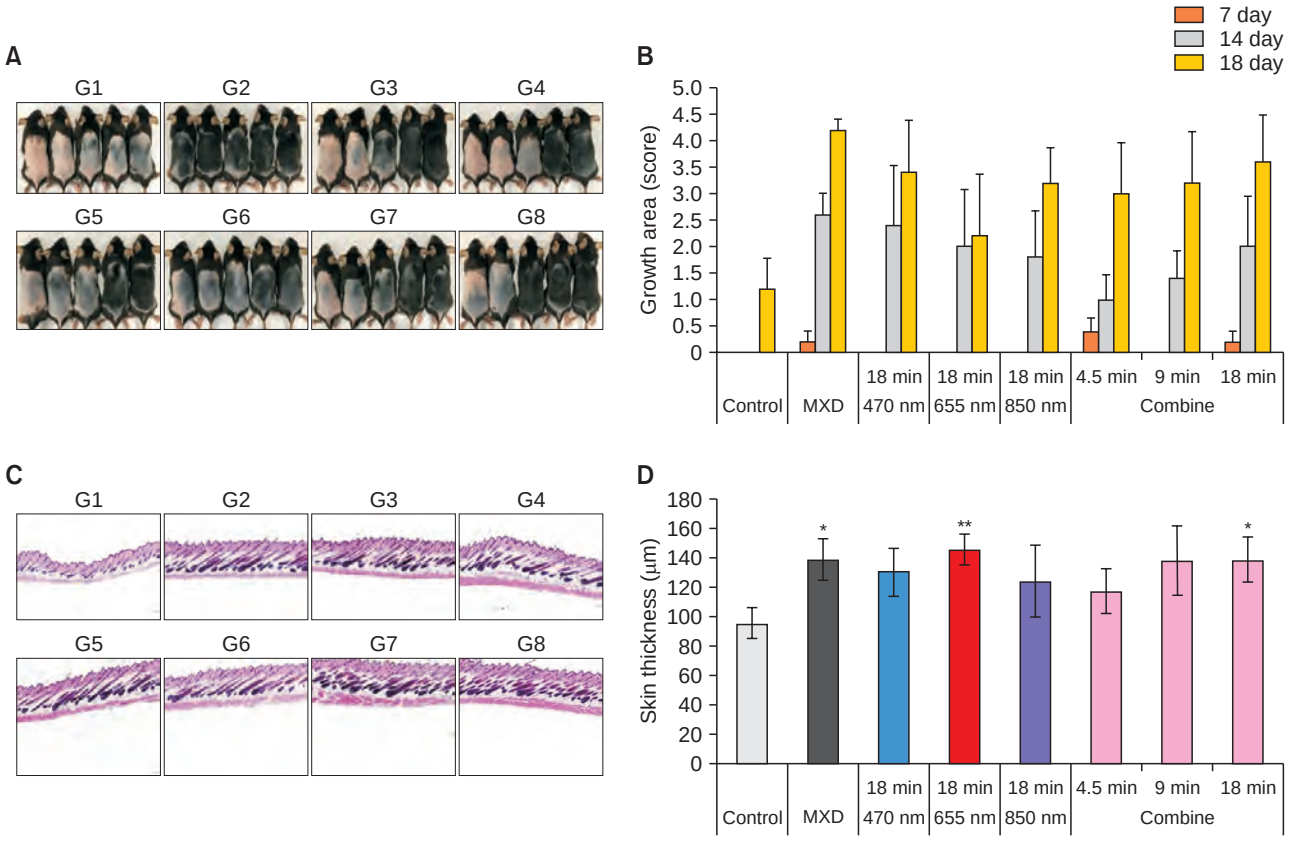

Fig. 3. Effects of photobiomodulation (PBM) therapy on hair follicles in telogen stage in C57BL/6J mice. The dorsal skin of C57BL/6 mice was treated as follows: untreated control, topical 3% minoxidil (MXD), or each PBM condition after 3, 10, 14, and 18 days (G1, control; G2, 3% MXD; G3, 470 nm, 18 minutes; G4, 850 nm, 18 minutes; G5, 650 nm LED/660 nm LD; G6, combine, 4.5 minutes; G7, combine, 9 minutes; G8, combine, 18 minutes). (A) Physical images and (B) after depilation, the dorsal skin of C57BL/6 mice was treated as follows: the untreated control, topical 3% MXD, or each PBM condition after 3, 10, 14, and 18 days. (B) Hair growth scores were evaluated using a scoring index (0 = no growth, 1 = up to 20% growth, 2 = 20%-40%, 3 = 40%-60%, 4 = 60%-80%, and 5 = 80%-100%). Hair growth was quantified using ImageJ (version 1.47, National Institutes of Health) (n = 5). Values are presented as mean ± standard error of the mean (SEM). n = 5/mouse. (C) Representative histology from five animals is shown: H&E stain, original magnification, ×200. (D) Skin thickness (defined as the distance from the epidermal granular layer to the top edge of the panniculus camosus) measurement. Values are presented as mean ± SEM (n = 5/mouse; *p < 0.05, **p < 0.01 vs. untreated control).

removal paste approach. We confirmed the variations in hair growth rate and mechanism for normal hair follicles based on the irradiation method of each wavelength using the model mentioned above. The device treatment did not result in bleeding, aberrant inflammatory reactions, dermal tissue necrosis, or skin surface damage. Depending on the LED irradiation time, an effect beyond the additive effect is expected as a result of measuring the hair growth area using the growth phase induction model. Notably, after 4 days of therapy at each wavelength, the MXD and the combined 4.5 and 18 minutes irradiation groups showed some newly developed hair on their backs (Fig. 3A, B). After 18 days of treatment, the newly grown hair coverage area reached 80%.

Effects on the development of anagen-phased hair follicle

The skin was divided horizontally on the skin's surface for this investigation, and the maximal cross-sectional area of a hair follicle was determined at that location. The entire skin layer expanding as it grows up to the fat layer is a characteristic of the hair growth phase. The skin's thickness and hair follicle length were increasing by day 18. Skin irritation caused by the irradiation was not seen histologically, indicating that the safety of the test device. The hair follicle count and skin thickness were measured microscopically. The results showed that the 650 nm LED/660 nm LED and combined 18 minutes groups were the most efficient in the effective wavelength range associated with hair follicle elongation (Fig. 3B). Significantly,

www.kci.go.kr

PBM also increased the skin thickness of hair follicles, indicating the induction of the anagen phase (Fig. 3C, D). These findings imply that PBM stimulated the anagen phase in telogen-phase animals, hence stimulating hair growth.

PBM therapy induced the expression of Shh and OPN3

We used immunohistochemical analysis to assess the signaling mechanism behind the induction of the anagen phase in each PBM group. It was possible to verify the increased expression of each of these proteins based on the staining intensity for each test group. Additionally, by comparing the groups, verification of the mono-PBM

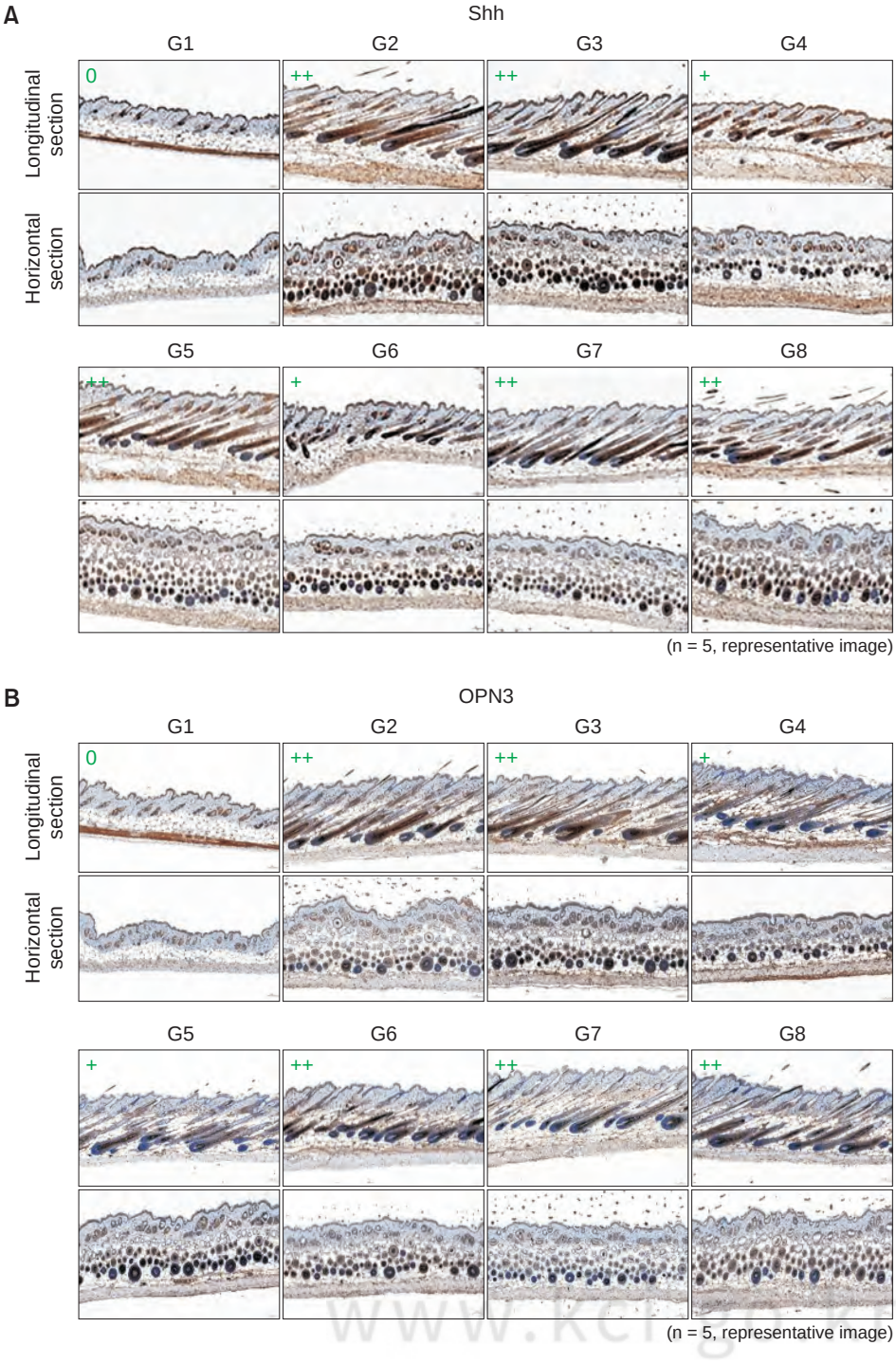

Fig. 4. Representative sections of skin tissues of C57BL/6J mice stained for (A) Shh and (B) OPN3. Dorsal skin biopsies were taken after 18 days and immunohistochemically stained, with 3,3′-diaminobenzidine as chromogen with hematoxylin counterstain. G1, control, G2, 3% minoxidil; G3, 470 nm, 18 minutes; G4, 850 nm, 18 minutes; G5, 650 nm LED/660 nm LD; G6, combine, 4.5 minutes; G7, combine, 9 minutes; G8, combine, 18 minutes. Two independent, blinded pathologists evaluated each serial section. Each pathologist assigned each section a score according to the following scale: 0, negative control; +, moderately increased staining; ++, considerably increased staining, based on the percentages of stained cells in each category. Representative images of IHC staining n = 10 mice per group. Original magnification, ×200.

www.kci.go.kr

group having a lower overall expression of hair growth-related proteins such as Shh and OPN3 was possible (Fig. 4). These findings reveal that PBM stimulates the growth of hair follicles via the β-catenin pathway and that PBM activates specific mechanisms during the anagen phase. When combined, these data point to the possible role of PBM in the activity that promotes hair growth.

DISCUSSION

Light therapy is used to treat a wide range of diseases, particularly hyperproliferative skin conditions such as psoriasis, acne, and keratosis. Both clinical and physical irradiation characteristics affect the results of PBM. As a result, the effect that a mixture of radiation, applied simultaneously or sequentially, has on tissues and cells differs from those brought about by radiation from a mono-wavelength. The link between the photoacceptors and superficial and deep tissue absorption can be attributed to this [13]. Therefore, integrating the radiation from low-power lasers and LEDs into devices that produce different wavelengths could be a novel way to enhance the positive effects of PBM. More research is needed to assess the therapeutic benefits of these devices over mono-wavelength devices.

Light penetration into the skin illustrates the depth to which wavelengths penetrate human skin. In general, the longer the wavelength, the deeper the penetration. Depending on the type of tissue, the penetration depth is <1 mm at 400 nm, 1-6 mm at 630 nm, and maximal at 700-900 nm. In particular, blue light, which forms a large percentage of ultraviolet A light (380-400 nm) and frequently has a wide variety of wavelengths, has been used in light treatment more frequently in recent years. Furthermore, many blue light-emitting lamps are advertised as improving well-being, emitting blue light at a maximum of 400-440 nm [14]. We conducted a thorough investigation using LED arrays to assess the impact of various wavelengths (412-940 nm) on skin cells. Several studies have shown that this may be related to OPN3 expression, which is involved in hair follicle growth [15].

Additionally, radiation has greater penetration through superficial skin layers and decreased spreading and absorption by tissue photoacceptors; therefore, radiation inside the therapeutic window elicits PBM. Longer wavelengths (780-950 nm) are preferable for treating disorders affecting deeper tissues, whereas shorter wavelengths (600-700 nm) are thought to be the best for treating diseases in superficial tissue [16].

Superficial and deep tissues can absorb multiple wavelengths at differing rates; therefore, the favorable effects of these wavelengths can be linked to differences in absorption levels. Owing to the varying molecules and composition of tissues, radiation penetration into tissues depends on absorption and scattering. When the radiation wavelength increases, both absorption and scattering dramatically decrease. For example, the penetration depth of NIR light reaches its maximum at about 810 nm. However, water plays a significant role as an absorber at longer wavelengths, and radiation penetration decreases once again [17].

We aim to determine the extent to which dermal papilla cells respond to each wavelength of LED. This study also evaluated mRNA expression to better understand the mechanisms underlying hair growth and inhibitory factors in hDPCs. It was verified that there was a significant increase in the expression ratio of ALP, Shh, VEGF, and OPN3 in the mono- and combined PBM treatment groups compared to the control group. The study's findings support the hypothesis that hair development and ALP, Shh, VEGF, and OPN3 expression are strongly correlated. The production of VEGF and ALP is critical for blood vessel development surrounding hair follicles. The capillaries surrounding hair follicles provide vital nutrients for the development and proliferation of the hair follicles.

This investigation verified that the blue wavelength causes an increase in the expression of VEGF and ALP. Thus, blue wavelengths may help develop and expand hair follicles. The use of several wavelengths for irradiation significantly increased shh for keratinocyte differentiation when compared to mono-wavelengths. Consequently, the complex wavelength will promote hair growth and contribute to the development of early hair follicles.

According to animal testing results, skin thickness measurements by group revealed statistical significance in all survey groups; in the case of the G2, G4, and G5 test groups, different skin layers have been suggested to be stimulated to encourage the creation of thick hair. When triggering the growth phase from the telogen stage, Shh controls the hair cycle and the growth of hair follicles. Although analyzing is challenging at the early stage of hair follicle growth, Shh expression is generally well stimulated depending on the irradiation period. Also, OPN3 is primarily expressed in hair follicles during the growth phase, helps to maintain the growth phase, and is linked to the development of outer root sheath (ORS) cells and the thickness of hair follicles. As a result, blue wavelengths stimulate the expression of these proteins, even though the direct comparison was challenging

www.kci.go.kr

while the hair was developing. To obtain optimal target tissue effects, determining the best values for each of these factors and the combination of treatment times and radiation is necessary. Additionally, most of the studies conducted to date have only used small sample numbers and/or brief treatment durations. These restrictions make it more challenging to understand and improve the effectiveness of LED treatments. Subsequent research efforts should elucidate the facilitative impact on the growth cycle within suitable models and associated mechanisms.

The study's results have been reported in fluence only, fluence and irradiance, fluence and time, and irradiance and time, among others. Occasionally, the dosage was not stated. Two of these factors enable the acquisition of the third since the fluence is the product of the irradiance with time. Comparing various studies carried out with mice, humans, reconstructed human epidermis, or different cells is also challenging. Our research still has several unresolved concerns, such as whether the blue, red, or infrared wavelength is the ideal wavelength for a light source, how long the light continues for, etc., which need to be optimized in our future work. In summary, multiple-wavelength LEDs expedited the telogen hair follicle regeneration compared to monotherapy and enhanced hair development.

ORCID

Soo Min Kim, https://orcid.org/0000-0003-2508-9593
Tae-Rin Kwon, https://orcid.org/0000-0002-9892-7714
Dong Wook Moon, https://orcid.org/0000-0001-5564-2893
Jungwook Kim, https://orcid.org/0000-0003-3639-8391
Rae Hyun Lim, https://orcid.org/0009-0003-6851-8316
Jungkwan Lee, https://orcid.org/0000-0002-5365-4740
So Young Lee, https://orcid.org/0000-0002-4119-5356
Ka Ram Kim, https://orcid.org/0000-0002-4308-8589
Young Gue Koh, https://orcid.org/0000-0002-6376-0328
Hye Sung Han, https://orcid.org/0000-0002-3556-0740
Sun Young Choi, https://orcid.org/0000-0003-0248-7708
Kwang Ho Yoo, https://orcid.org/0000-0002-0137-6849

AUTHOR CONTRIBUTIONS

Conceptualization: SMK, TRK. Data curation: DWM, RHL. Formal analysis: JK. Investigation: SMK, TRK. Methodology: SMK. Project administration: KHY. Software: JL, SYL. Validation: KRK, YGK. Visualization: HSH, RHL. Writing–original draft: TRK, KHY, SYC. Writing–review & editing: all authors.

CONFLICT OF INTEREST

Kwang Ho Yoo is the Editor-in-Chief, Tae-Rin Kwon and Hye Sung Han are editorial board members of the journal, but they were not involved in the review process of this manuscript. Otherwise, there is no conflict of interest to declare.

FUNDING

None.

DATA AVAILABILITY

Contact the corresponding author for data availability.

ACKNOWLEDGMENTS

None.

SUPPLEMENTARY MATERIALS

None.

REFERENCES

1. Dompe C, Moncrieff L, Matys J, Grzech-Leśniak K, Kocherova I, Bryja A, et al. Photobiomodulation-underlying mechanism and clinical applications. J Clin Med 2020;9:1724.
2. Nie F, Hao S, Ji Y, Zhang Y, Sun H, Will M, et al. Biphasic dose response in the anti-inflammation experiment of PBM. Lasers Med Sci 2023;38:66.
3. Dong J, Xiong D. Applications of light emitting diodes in health care. Ann Biomed Eng 2017;45:2509-23.
4. Heiskanen V, Hamblin MR. Photobiomodulation: lasers vs. light emitting diodes? Photochem Photobiol Sci 2018;17:1003-17. Erratum in: Photochem Photobiol Sci 2018;18:259.
5. Pruitt T, Carter C, Wang X, Wu A, Liu H. Photobiomodulation at different wavelengths boosts mitochondrial redox metabolism and hemoglobin oxygenation: *lasers* vs. *light-emitting diodes in vivo*. Metabolites 2022;12:103.
6. Schütz R. Blue light and the skin. Curr Probl Dermatol 2021; 55:354-73.
7. Campiche R, Curpen SJ, Lutchmanen-Kolanthan V, Gougeon S, Cherel M, Laurent G, et al. Pigmentation effects of blue light irradiation on skin and how to protect against them. Int J Cosmet Sci 2020;42:399-406.
8. Avci P, Gupta A, Sadasivam M, Vecchio D, Pam Z, Pam N, et al. Low-level laser (light) therapy (LLLT) in skin: stimulating, healing, restoring. Semin Cutan Med Surg 2013;32:41-52.

www.kci.go.kr

9. Tsai SR, Hamblin MR. Biological effects and medical applications of infrared radiation. J Photochem Photobiol B 2017;170:197-207.
10. Kwon TR, Moon DW, Yoon BH, Lee SJ, Lee SJ, Hwang J, et al. Hair growth promotion by photobiomodulation therapy using different parameters: animal study. Med Lasers 2023;12:34-43.
11. Andreasen E. Cyclic changes in the skin of the mouse. Acta Pathol Microbiol Scand 1953;32:157-64.
12. Kwon TR, Oh CT, Park HM, Han HJ, Ji HJ, Kim BJ. Potential synergistic effects of human placental extract and minoxidil on hair growth-promoting activity in C57BL/6J mice. Clin Exp Dermatol 2015;40:672-81.
13. Ablon G. Phototherapy with light emitting diodes: treating a broad range of medical and aesthetic conditions in dermatology. J Clin Aesthet Dermatol 2018;11:21-7.
14. Nitayavardhana S, Manuskiatti W, Cembrano KAG, Wanitphadeedecha R. A comparative study between once-weekly and alternating twice-weekly regimen using blue (470 nm) and red (640 nm) light combination LED phototherapy for moderate-to-severe acne vulgaris. Lasers Surg Med 2021;53:1080-5.
15. Buscone S, Mardaryev AN, Raafs B, Bikker JW, Sticht C, Gretz N, et al. A new path in defining light parameters for hair growth: discovery and modulation of photoreceptors in human hair follicle. Lasers Surg Med 2017;49:705-18.
16. Noé C, Pelletier-Aouizerate M, Cartier H. [LED lights in dermatology]. Ann Dermatol Venereol 2017;144:301-14. French.
17. Brownell J, Wang S, Tsoukas MM. Phototherapy in cosmetic dermatology. Clin Dermatol 2016;34:623-7.

How to cite this article: Kim SM, Kwon TR, Moon DW, Kim J, Lim RH, Lee J, Lee SY, Kim KR, Koh YG, Han HS, Choi SY, Yoo KH. Multiple-wavelength radiation promotes hair growth by enhancing the early stages of hair follicle development in human dermal papilla cells and C57BL/6 mice. Med Lasers 2024;13:35-46. https://doi.org/10.25289/ML.24.004

www.kci.go.kr